

Electronic Supplementary Information

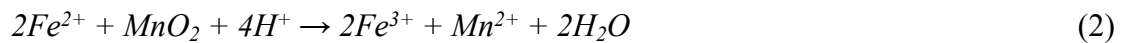
Experimental Section

Synthesis process of materials

Materials. All chemicals purchased from Aladdin were of analytical purity and used without further purification.

Synthesis of MnO₂ nanosheets on Diatomite (D). The diatomite@MnO₂ was assembled by a facile hydrothermal method. 40 mg diatomite and 35 mL 0.05 M KMnO₄ solution were added into a 50 mL autoclave. The Teflon-lined stainless steel autoclave was kept at 160 °C for 24 h in an oven. The samples were washed with distilled water and then dried at 60 °C for several hours. Finally, the MnO₂@diatomite were obtained.

Synthesis of FeOOH nanorods on Diatomite. The preparation of FeOOH nanorods are completed via a simple hydrothermal method which is a redox action from MnO₂ to FeOOH. Firstly, 80 mg D@MnO₂ and 0.01 M 70 mL FeSO₄•7H₂O mixed solvent containing distilled water and ethylene glycol (V_E/V_D =1/7) were moved into a Teflon-lined stainless steel autoclave and heated at 120 °C for 2 h in a rotating oven. Then, wash the solid precipitates with distilled water and dry at 60 °C for several hours. The D@α-Fe₂O₃ and D@γ-Fe₂O₃ were obtained by calcination in air at 350 °C and in N₂ at 500 °C for 2 h, respectively. The chemical reaction is shown in following Equation (1) and (2):



PPy coating on composites. The 200 mg samples (D@FeOOH, D@α-Fe₂O₃ and D@γ-Fe₂O₃) and 40 mg FeCl₃•6H₂O were dissolved into a number of distilled water. After tired evenly, the mixture was dried in a oven. Then, the solid-state mixture and 3 mL pyrrole were transferred into two beaker, separately. The beakers were put into a sealed container and heated at 60 °C for 24 h by a water bath kettle. Finally, the D@FeOOH@PPy was collected by centrifugal washing.

Material characterization

High resolution TEM (HRTEM) images were obtained on a JEOL-2100F TEM (JEOL, Japan) with an acceleration voltage of 200 kV. The crystallographic information and chemical compositions of the as-prepared nanostructures were established by powder X-ray diffraction (XRD, D/max 2500, Cu Kα), and they were analyzed with the JADE 6.0 software. The structures and morphologies of the as-prepared nanostructures

were measured by focused ion beam scanning electron microscopy (FIB/SEM, ZEISS AURIGA). The BET specific surface area was obtained by N₂ adsorption/desorption isotherms at 77 K (ASAP 2020 sorptometer). XPS spectra were acquired on a Physical Electronics ESCA 5600 spectrometer with a monochromatic Al K α X-ray source (power: 200 W/14 kV) and a multichannel detector (Omni IV).

Electrochemical measurement

Electrochemical measurements of the samples were tested by using an electrochemical workstation (CHI 660E) with a three-electrode and a two-electrode configuration in 1 M Na₂SO₄ electrolyte.

For three-electrode configuration, the active materials were used as a working electrode, and a Pt plate was used as a counter electrode, the standard calomel electrode (SCE) as a reference electrode. As for the working electrode, nickel foam (1 \times 1.5 cm²) was used for a current collector with 1 \times 1 cm² slurry on it, which is consist of active materials, carbon black and polyvinylidene fluoride (weight ratio=7:2:1) in N-methyl-2-pyrrolidone (NMP). The nickel foam with slurry was heated to evaporate the dissolvent in a vacuum oven at 120 °C for 12 h. All the samples were regarded as negative electrode with a potential of -0.8~0 V.

For the tests with a two-electrode configuration, the D@MnO₂@PPy was used as the positive material and the D@FeOOH@PPy was used as the negative material. The galvanostatic charge-discharge measurement has an expanding potential window of 1.6 V.

The electrochemical properties of the three-electrode and two-electrode configuration were tested by cyclic voltammetry (CV) at scan rates of 10 to 200 mV s⁻¹ and galvanostatic charge-discharge (GCD) at current densities of 0.5 to 5 A g⁻¹. The electrochemical impedance spectroscopy (EIS) experiments were carried out in the frequency range from 0.01 Hz to 100 kHz with a perturbation amplitude of 5 mV versus the open-circuit potential.

The specific capacitance C_m (F g⁻¹) and energy/power density are calculated by the following Equation (3-5):

$$C_m = \frac{I \times \Delta t}{m \times \Delta V} \quad (3)$$

$$E = 0.5 \times C_m \times \Delta V^2 / 3.6 \quad (4)$$

$$P = 3600 \times E / \Delta t \quad (5)$$

where I (A) is the discharging current, Δt (s) is the discharging time, ΔV (V) is the potential window, m is the weight of active materials, E is the energy density and P is the power density.

The formula of mass loading between the positive and negative electrodes in two-electrode configuration is calculated by the following Equation (6) and (7):

$$Q = C \times \Delta V \times m \quad (6)$$

$$\frac{m_p}{m_n} = \frac{C_n \times \Delta V_n}{C_p \times \Delta V_p}$$

(7)

Where Q is quantity of electric charge, C is the specific capacitance, ΔV is the potential window, m is the weight of active materials, p is positive and n is negative.

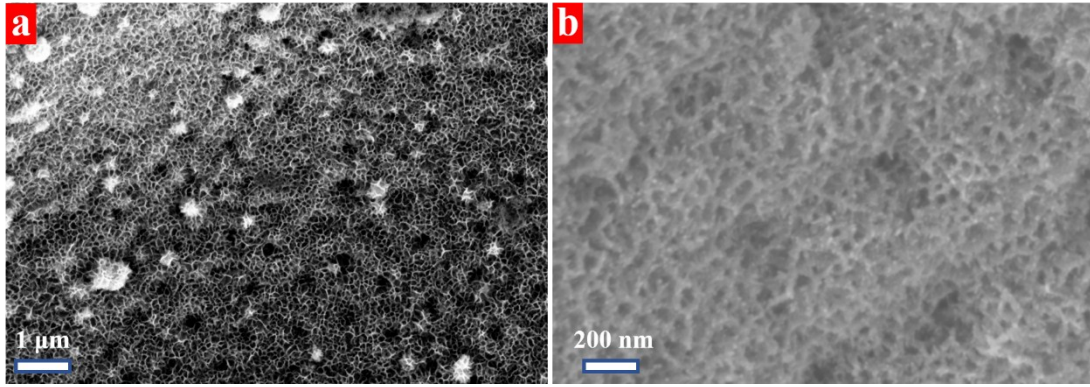


Fig. S1 The SEM image of (a) D@MnO₂ nanosheets and (b) D@FeOOH nanorods materials.

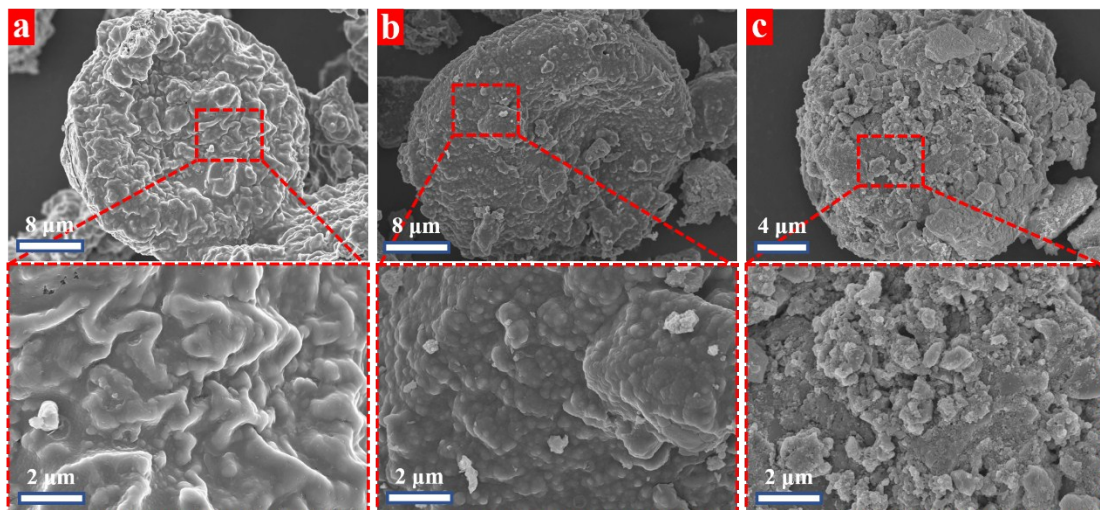


Fig. S2 The SEM images and corresponding magnified images of (a) D@PPy, (b) D@ α -Fe₂O₃@PPy and (c) D@ γ -Fe₂O₃@PPy.

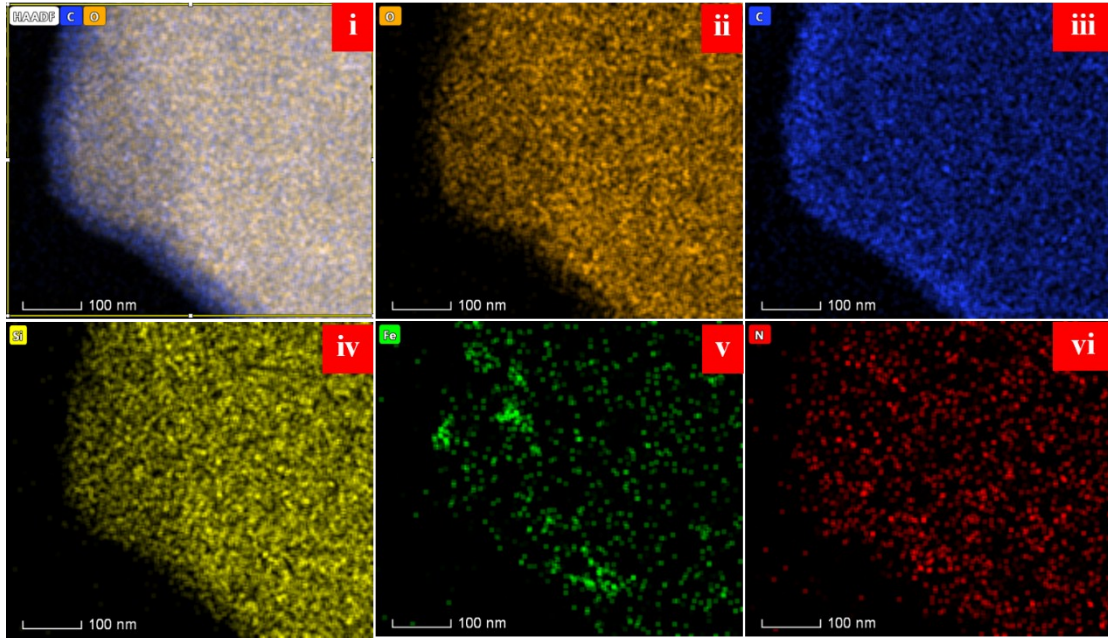


Fig. S3 The EDS mapping of D@FeOOH@PPy: (i) C and O; (ii) O; (iii) C; (iv) Si; (v) Fe; (vi) N.

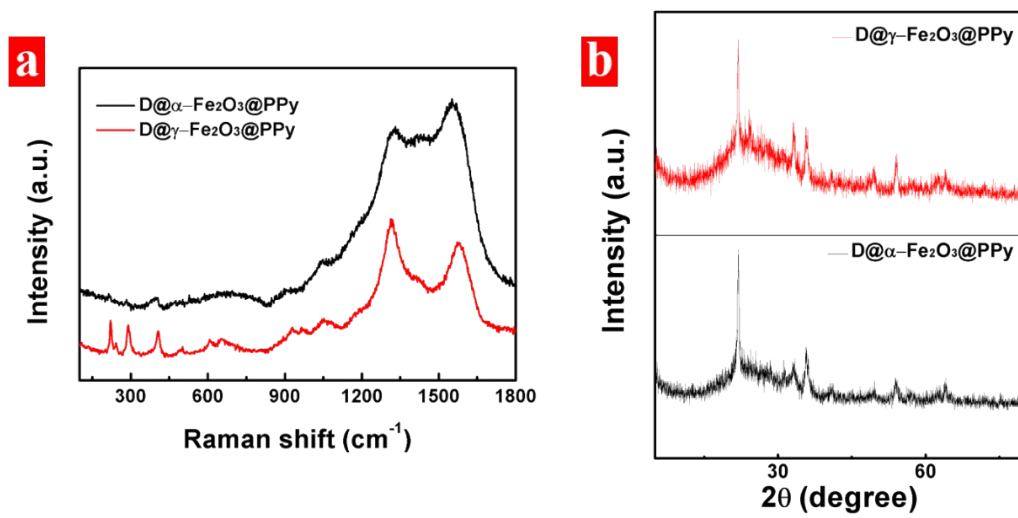


Fig. S4 The (a) Raman and (b) XRD of D@ α -Fe₂O₃@PPy and D@ γ -Fe₂O₃@PPy

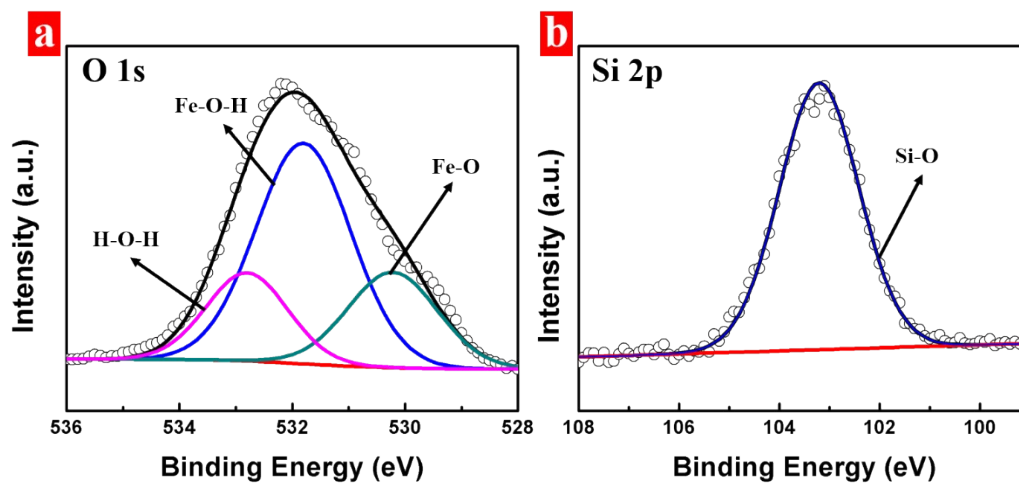


Fig. S5 The XPS of D@FeOOH@PPy : (a) O 1s and (b) Si 2p

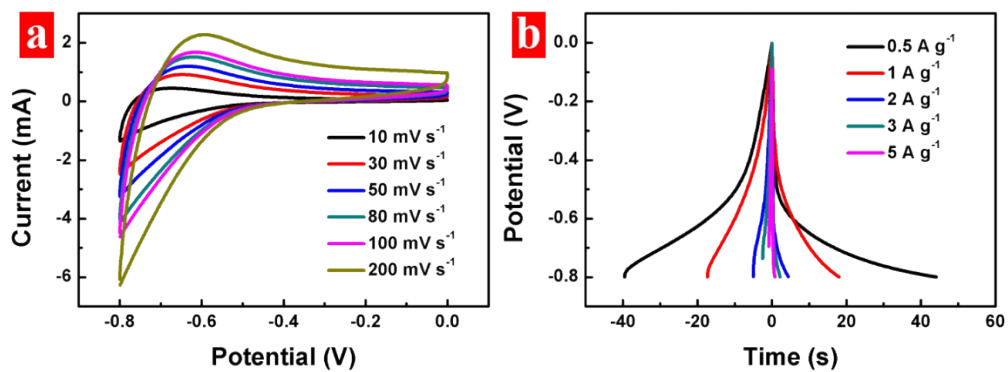


Fig. S6 The (a) CV curves at different scan rates and (b) CC curves at different current density of D@FeOOH.

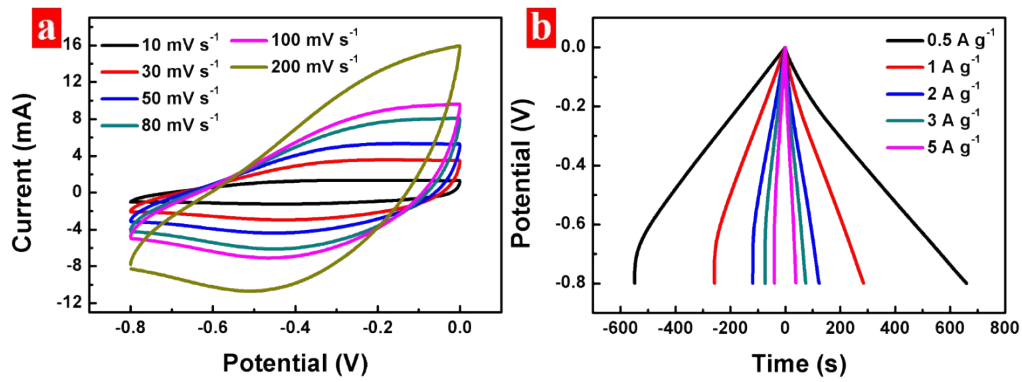


Fig. S7 The (a) CV curves at different scan rates and (b) CC curves at different current density of D@FeOOH@PPy.

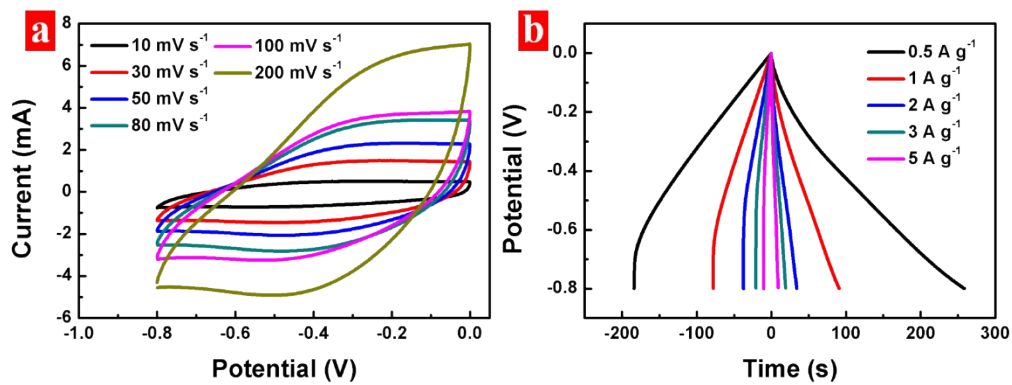


Fig. S8 The (a) CV curves at different scan rates and (b) CC curves at different current density of D@ α -Fe₂O₃@PPy.

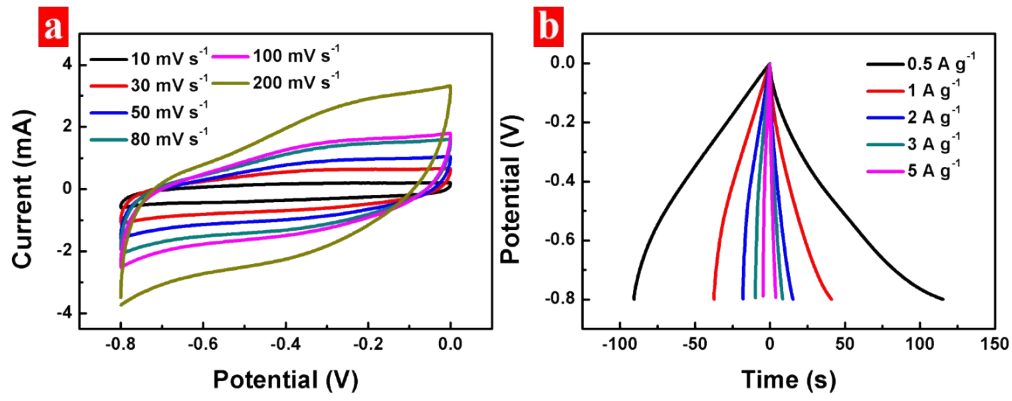


Fig. S9 The (a) CV curves at different scan rates and (b) CC curves at different current density of D@ γ -Fe₂O₃@PPy.

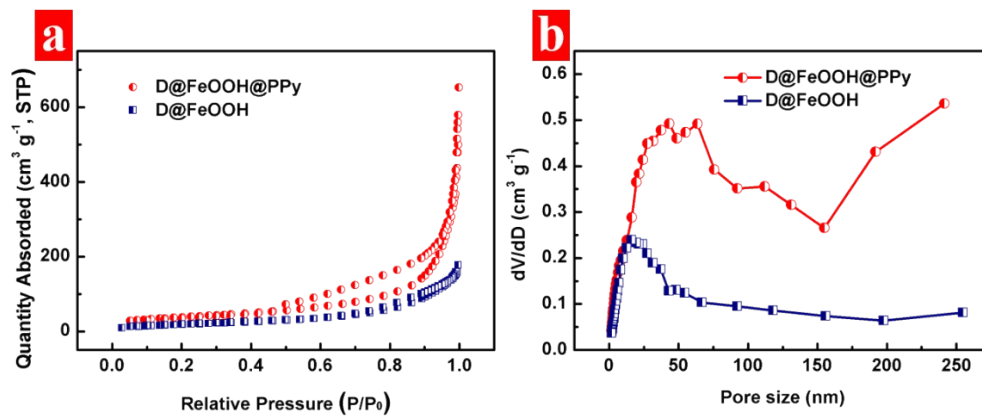


Fig. S10 The (a) N₂ adsorption/desorption isotherms and (b) Pore size distribution curves of D@FeOOH@PPy and D@FeOOH.

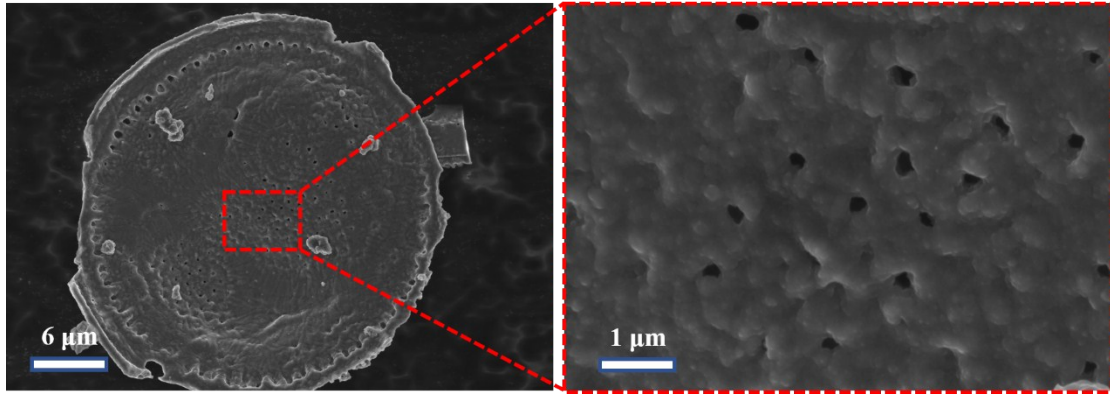


Fig. S11 The SEM image of D@FeOOH@PPy electrode material after 10000 cycles with low and high manganification.

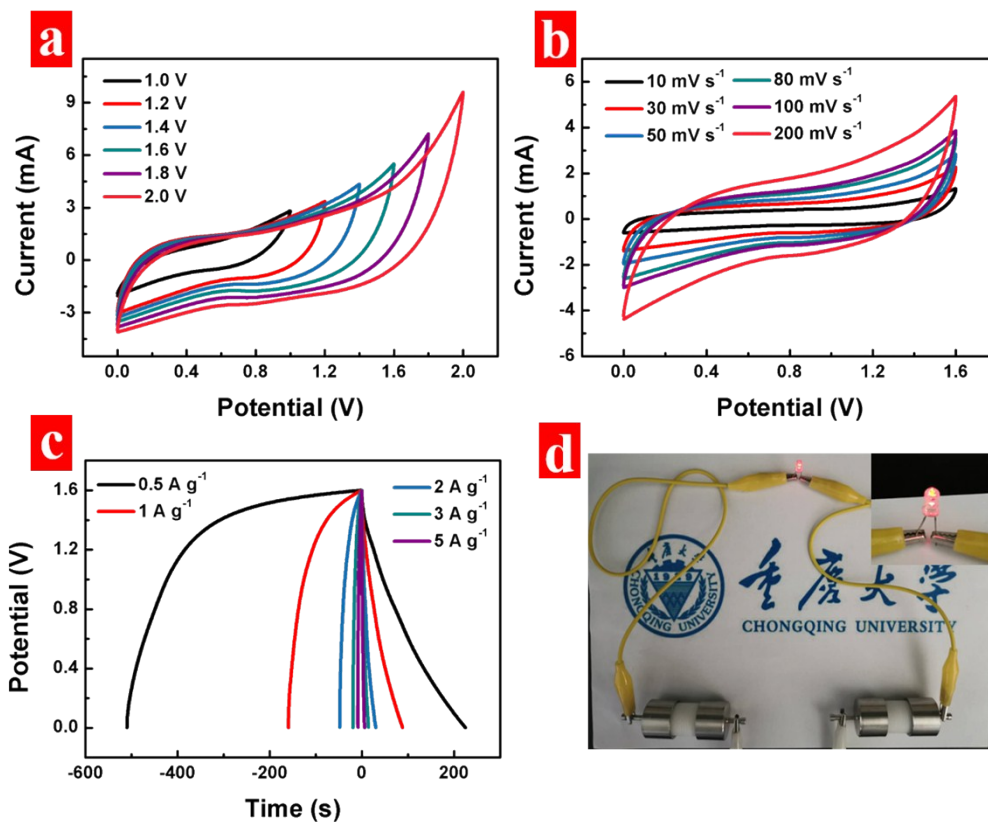


Fig. S12 (a) CV curves of D@FeOOH@PPy//D@MnO₂@PPy with different potential. (b) CV curves of D@FeOOH@PPy//D@MnO₂@PPy with different scan rates. (c) CC curves of D@FeOOH@PPy//D@MnO₂@PPy with different current densities. (d) The red LED lighted by the device.